Centrifuge model tests on soil desaturation as a liquefaction countermeasure

Essais de modèle centrifuge sur la désaturation du sol comme une contremesure de la liquéfaction

J. Takemura, R. Igarashi & J. Izawa
Tokyo Institute of Technology, Japan

M. Okamura & M. Masuda
Ehime University, Matsuyama, Japan

ABSTRACT

In this study a series of centrifuge model test has been conducted to investigate the mechanical behavior of the submerged but partially saturated sand during earthquake. In the centrifuge tests, an attempt was made to prepare partially saturated model sand by lowering and regaining ground water table under 50g centrifugal acceleration. The process of desaturation was monitored by Time Domain Reflectometer (TDR) and pore pressure transducers (PPT). A shaking test of the model was then conducted for the sand with a gravity type structure on the top to study the applicability of soil desaturation as a liquefaction countermeasure.

RÉSUMÉ

Dans cette étude, une série d'essai de modèle centrifuge a été réalisée pour étudier le comportement mécanique du sable submergé mais partiellement saturé pendant le tremblement de terre. Dans les essais de centrifuge, une tentative a été prise pour préparer le modèle de sable partiellement saturé en baissant et regagnant la nappe d'eau souterraine sous l'accélération centrifugeuse de 50g. Le processus de la désaturation a été contrôlé par le réflectomètre (TDR) et le transducteur de pression (PPT). Un essai de secouage sur modèle a été puis mené pour le sable désaturé avec une structure de type gravitaire sur le sommet pour étudier l'applicabilité de la désaturation du sol comme une contremesure de la liquéfaction.

Keywords: soil liquefaction, desaturation, centrifuge model tests

1 INTRODUCTION

Effects of degree of saturation, S_r, on liquefaction of sand have been mostly studied through laboratory tests. In early research works, the negative effects of incompleteness of the saturation were investigated to avoid the undesirable unsaturated condition which resulted in overestimation of the liquefaction resistance (e.g., Martin et al., 1978). Recently the positive effects of partial saturation on the liquefaction resistance have been investigated to discuss the applicability of soil desaturation as a liquefaction countermeasure by many researchers using laboratory tests and field tests (e.g., Yoshimi et al, 1989; Tsukamoto et al., 2002; Okamura and Soga, 2006). Okamura and Soga (2006) found a unique relationship between the liquefaction resistance ratio (R_u/R_s, where R_u and R_s are liquefaction resistance of unsaturated and saturated soils respectively) and the potential volumetric strain ε_v^* defined by the following equation.

$$\varepsilon_v^* = \frac{\sigma_c'}{p_0 + \sigma_c'}\left(1 - S_r\right)\frac{e}{1+e} \tag{1}$$

where σ_c', p_0, and e denote the effective confining pressure, the absolute pressure of the fluid and the void ratio of soil respectively.

Centrifuge modeling has been used as a useful approach in the study of soil liquefaction, especially for verification of countermeasures against liquefaction (e.g., Kimura et al, 1997). Equation (1) implies that that effect of the degree of saturation cannot be well represented in small scale models at 1g but centrifuge models. Furthermore, the capillary rise can be well scaled in the centrifuge model, which is crucial in the simulation of lowering the ground water table as a method of soil desaturation (Figure 1).

In the centrifuge model test of this study, an attempt was made to prepare partially saturated model sand with ground water table at the ground surface. A shaking test of the sand with a footing was then conducted to study the applicability of soil desaturation as a liquefaction countermeasure.

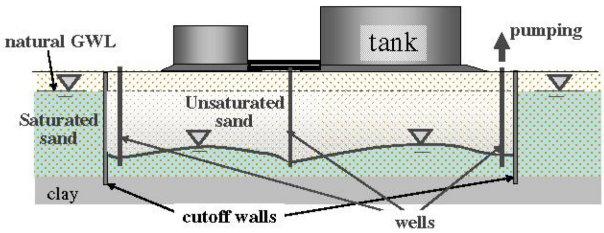

Figure 1. Desaturation of liquefiable soils by groundwater lowering.

2 CENTRIFUTE MODEL TESTS

2.1 *Soils used for tests*

Two types of silica sand with properties shown in Table 1 were used for the tests. In centrifuge modeling, viscous liquids are often used as pore-fluid to overcome mismatch in the similitude concerning seepage and dynamic events. However, to avoid uncertainty in the mechanical behavior of unsaturated sand with such viscous liquids, fine silica sand (No.8) and coarse sand (No.3) were used as the materials for the liquefiable sand and bottom drainage layer respectively with water as the pore-fluid in this study. In the centrifugal field of 50g, the permeability coefficients of the two silica sands in prototype scale are 50 times those in 1g as shown in Table 1. Capillary pressure - Sr curve of Silica sand No.8 is shown in Figure 2. Air entry value of the silica sand is about 5kPa.

In Figure 3 liquefaction curves obtained from cyclic triaxial tests on Silica sand No.8 with Dr=60% are shown together with the curves obtained from FEM code LIQCA (Oka et al.,). Figure 4 depicts the relationship between the potential

Proceedings of the 17[th] International Conference on Soil Mechanics and Geotechnical Engineering
M. Hamza et al. (Eds.)

doi:10.3233/978-1-60750-031-5-502

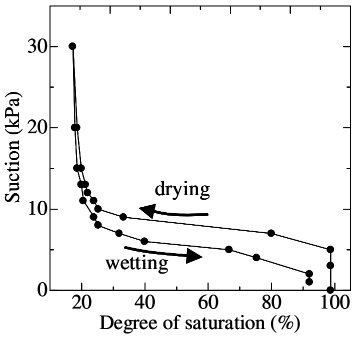

Figure 2. Capillary pressure and degree of saturation curve : Silica sand No.8.

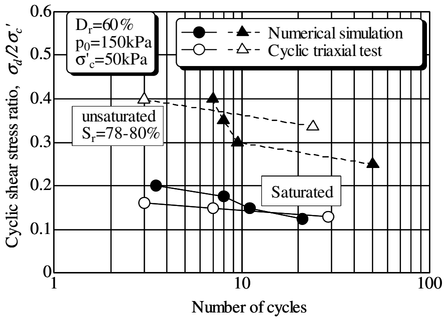

Figure 3. Relationship between cyclic stress ration and number of cycles: Silica sand No.8.

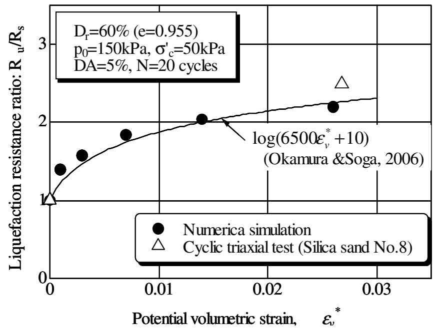

Figure 4. Relationship between potential volumetric stain and liquefaction resistance ratio.

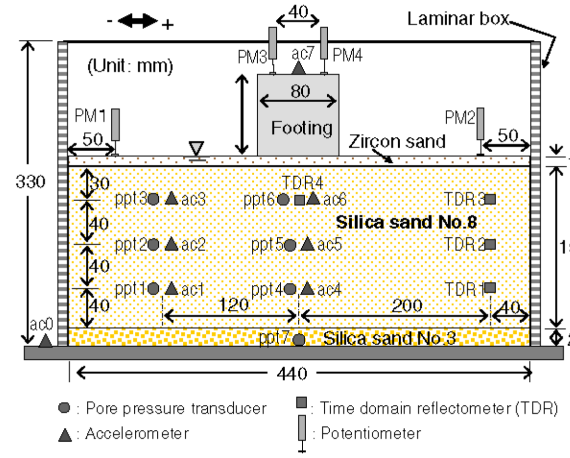

Figure 5 (a). Test setup and location of sensors in the model.

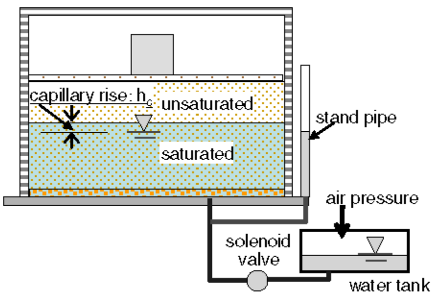

Figure 5 (b) Control of ground water level in the model.

volumetric strain (ε_v^*) and the liquefaction resistance ratio. In the figure, relationship proposed by Okamura and Soga (2006) are also shown. Liquefaction resistance for 80% saturation is about 2.5 times greater than that for full saturation.

Table 1 Properties of silica sands used

	No.8	No.3
Specific gravity: G_s	2.65	2.56
Mean particle size: D_{50} (mm)	0.100	1.47
Particle size: D_{10} (mm)	0.041	1.21
Coefficient of uniformity: U_c	2.93	1.26
Max. void ratio: e_{max}	1.333	0.971
Min. void ratio: e_{min}	0.703	0.702
Permeability coef.: k (m/sec)	2.0 x 10^{-5}	4.6x 10^{-3}
(k in prototype scale with 50g)	(1.0 x 10^{-3})	(2.3 x 10^{-1})

2.2 *Model preparation and test procedures*

A shear box made of aluminum with inner sizes of 440mm in width, 150mm in breadth and 310mm in height was used for the tests. Silica sand No.3 was first placed as the bottom drainage layer by compacting with a wooden rod and a dry layer of Silica sand No.8 was made by air pluviation with Dr=60%. 10mm thick Zircon sand was laid on the surface of the silica sand to give the surcharge pressure of 10kPa in 50g. During the sand preparation, various sensors were placed at the location shown in Figure 5(a). The model ground was saturated in a vacuum tank by introducing deaired water from the bottom of the box. After saturating the sand, a model footing made of solid aluminum with the dimensions of 80mm in width, 80mm in height and 150mm in breadth was placed on the center of the ground surface carefully. Mass of the footing is 2.5kg, giving the base contact pressure, p_f =100kPa in 50g. The model was then taken to Tokyo Tech Mark III Centrifuge and mounted on the shaker (Takemura et al. 2002). Potentiometers were installed at the position shown in Figure 5(a) and centrifugal acceleration was increased up to 50g.

After confirming the equilibrium condition in the model, the water was drained from the bottom to the water tack by opening the solenoid valve (Figure 5(b)). The valve was closed when the ground water level (GWL) in the standpipe lowered to the bottom of the sand layer. Achieving stationary reading of TDR sensor, the water was recharged from the bottom by applying air pressure to the water tank and opening the valve.

Confirming no change in the reading of TDR sensors and PPTs after the water table recovered to the original level, horizontal sinusoidal waves with frequency of 100Hz were applied to the model for 0.2 sec. Three tests were conducted in this study with the condition shown in Table2.

Table 2 Test condition

Test code	S10	U15	U10
Relative density Dr (%)	62	2.65	2.56
Degree of saturation* (%)	100	93	92
Input acceleration amplitude(g)	10	13	10

*: evaluated from the water remained in the water tank

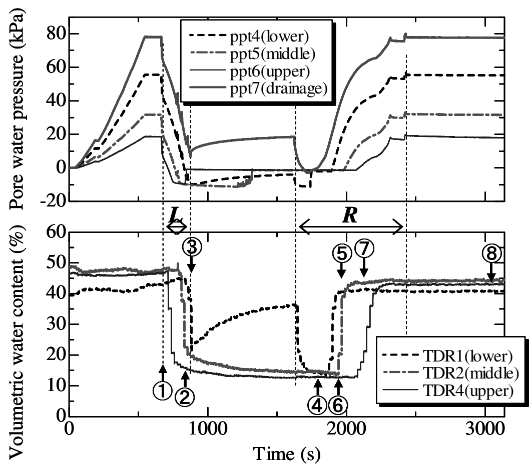

Figure 6. Variation of pore pressure and volumetric water content in desaturation process: U15.

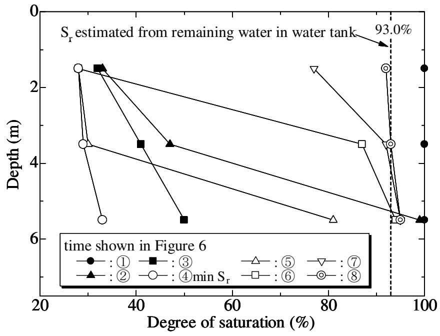

Figure 7. Depth profile of degree of saturation in desaturation process: U15.

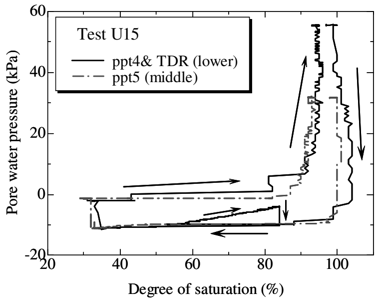

Figure 8. Variation of pore water pressure with S_r.

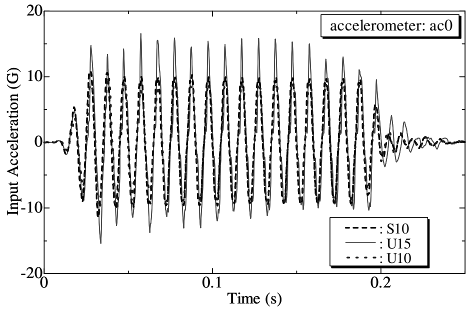

Figure 9. Input base acceleration measured by ac0.

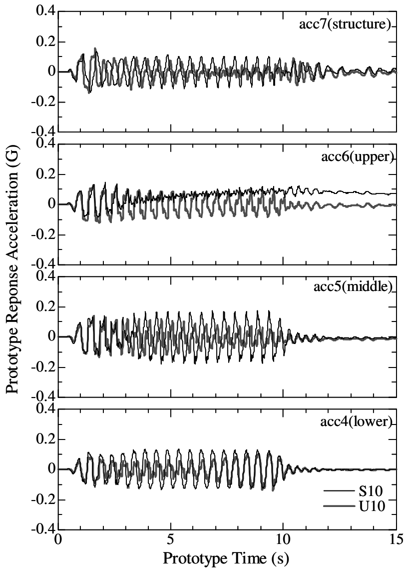

Figure 10. Observed acceleration beneath the footing.

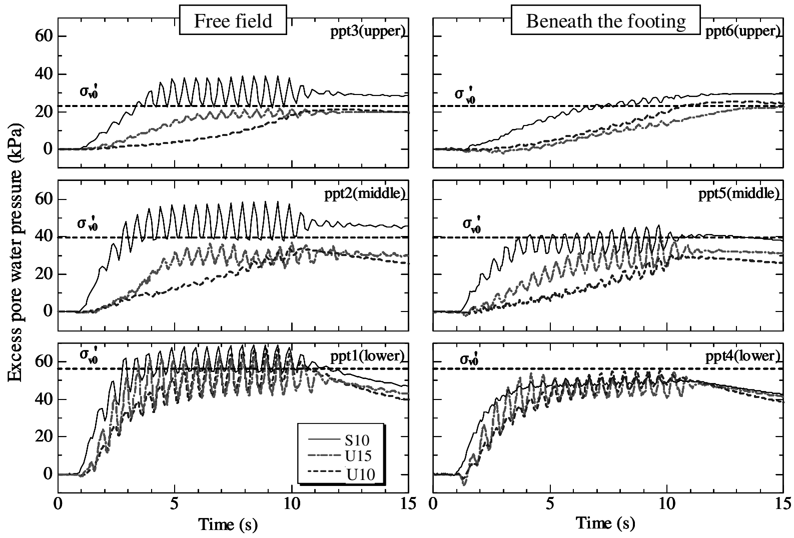

Figure 11. Variation of excess pore pressure in the model ground during shaking.

3 TEST RESULTS AND DISCUSSIONS

In the following discussion, test results are given in prototype scales except of Figures 6 and 9.

3.1 *Desaturation process*

Figure 6 shows the pore water pressures and volumetric water contents observed with PPT and TDR sensors during the desaturation process in U15. The variation of depth profile of S_r is depicted at various stages shown in Figure 7. The S_rs in the desaturation process were calculated from the water volumetric content assuming full saturation before lowering the water table. By lowering the GWL, S_r decreased to about 30% and recovered to 93% at the original GWT. S_r obtained in U10 was 92%. The potential volumetric strain for these S_rs with the same conditions shown in Figure 3 is 0.0086 and R_u/R_s estimated by the equation given in Figure 4 is 1.8. The variations of pore pressure with S_r are shown in Figure 8. From this figure, about 1m of capillary rise in the sand can be estiamted, which indicates that the same size of 1g model could be fully saturated by the capillary rise if the GWL is at the bottom of the sand. The sudden increase of pore water pressure is due to the limitation of capacity of PPT in measuring the suction.

3.2 *Shaking tests*

Input base accelerations measured by acc0 (Figure 5(a)) are shown in Figure 9.

3.2.1 *Acceleration response*

Horizontal accelerations observed by the vertical array of accelerometers at the center of model are compared for S10 and U10 in Figure 10. Clear attenuation was observed just beneath the footing in the saturated case (S10) but not in the unsaturated case (U10), while that of the footing is vice versa. It is hard to find the clear effect of partial saturation in the acceleration response. Complicated motion of footing might occur, which could not be captured by one accelerometer at the top.

3.2.2 *Pore water pressure behavior*

Observed excess pore water pressures (EPEP) during shaking are compared in Figure 11. In the figure effective vertical stress, σ'_{v0}, is shown. At the free field, EPWP reached to σ'_{v0} in early stage of motion at all depths for U10, implying the clear liquefaction. While for U10 and U15, generation of EPWP was more gradual, confirming the effect of partial saturation on the liquefaction resistance. It should be noted that the locations of PPT might be different from those targeted, which is considered as a reason of higher EPWP greater than σ'_{v0}. Large cyclic variation of EPWP in the free field is attributed to the cyclic load from the footing. Although the direct comparison is not possible between the free field and the portion underneath the footing because of different stress condition, similar positive effect of the partial saturation is also observed in EPWP underneath the footing as in the free field. The difference between saturated case and partially saturated cases is more eminent at the shallow portion, which is explained by the effect of absolute fluid pressure, p_0, on the potential volumetric strain in eq. (1), and difference of Sr in depth.

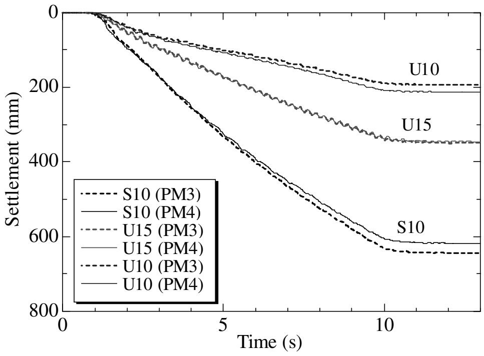

Figure 12. Settlements of the footing during shaking.

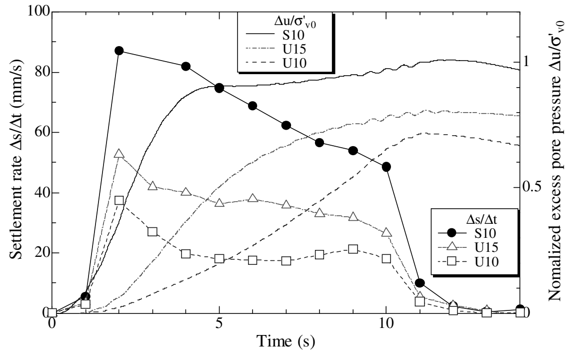

Figure 13. Variation of settlement rate of footing and normalized excess pore water pressure (PPT5) during shaking.

3.2.3 *Settlement behavior*

Observed settlements of the footing during shaking tests are shown in Figure 12. The settlement of U10 is about one third of that S10 and the settlement of U15 with input motion 50% greater than S10 and U10 is about one second of S10. Although the settlement rate is very different between the cases, it was slightly decreasing with time in S10 but gradually increasing with time in S10 as shown in Figure 13, which can be attributed to the delayed decrease of effective stress for U10. Clear effect of partial saturation on the differential settlement could not be confirmed in the tests. The settlement of the footing and free field during and after shaking are shown in Figure 14. In Figure 15 total settlement of the footing and free field are compared with fraction of those during and after shaking. Majority of the footing settlement took place during shaking, while the free field showed long term settlement after shaking. The ratio of the settlements after shaking to that during shaking in the free field is larger for the saturated case than the partially saturated cases and larger for U15 than U10. From these comparisons, it can be said that the extent of liquefaction highly influences the settlement after shaking in the free field.

4 CONCLUSIONS

The following conclusions can be drawn in this study.

1) Centrifuge modeling is a useful tool to simulate the desaturation process by lowering and recovering ground water table in sandy ground. With the conditions adopted in the study, the residual degree of saturation, S_r, was about 92-93%.
2) Pore water generation can be effectively sustained both at free field and underneath structure by the desaturation process even with relatively high S_r given in the above. The efficiency is more apparent in shallower depth than the deep one.

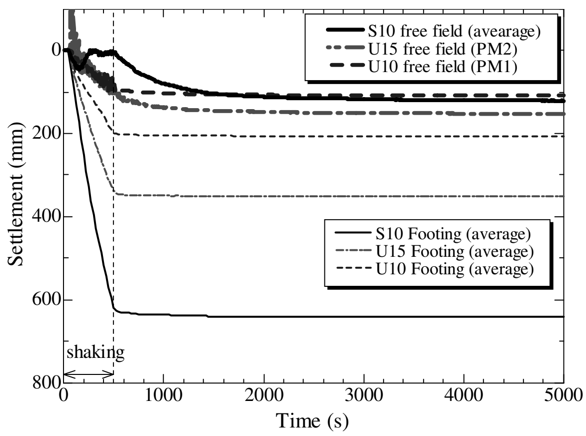

Figure 14. Settlements of the footing and free field during and after shaking.

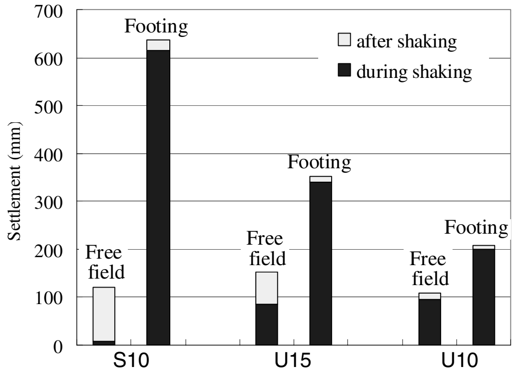

Figure 15. Settlements of the footing and free field.

3) Settlements of structure on partially saturated sand are much smaller than that of the saturated sand.
4) Although the centrifuge modeling is very useful for the study in saturated and unsaturated sand, there are still a lot of limitations, e.g., inconsistency of similitude about Bond number in micro scale. To verify the applicability of centrifuge and quantify the effect of desaturation, further tests with various conditions is recommended.

REFERENCES

Kimura, T., Takemura, J., Hirooka, H. and Okamura, M. (1997): Countermeasures against liquefaction of sand deposits with structures, *Proc. Intn. Conf. Earthquake Geotechnical Engineering, IS Tokyo 95*, Vol.3, 1203-1224.

Martin , G. R., Finn, W.D. L, and Seed, H. B.(1978): Effects of system compliance on liquefaction tests, *J. Geotech. Engrg. Div., ASCE,* 104(4), 463-479.

Oka, F., Yashima, A., Shibata, T., Kato, M., and Uzuoka, R. (1994): FEM-FDM coupled liquefaction analysis of a porous soil using an elasto-plastic model, *Applied Scientific Research*, Vol.52, 209-245.

Okamura, M. and Soga, Y. (2006): Effects of pore fluid compression on liquefaction resistance of partially saturated sand, *Soils and Foundations*, 46(5), 695-700.

Takemura, J., Takahashi, A. & Aoki,T.(2002):Development of horizontal-vertical 2D shaker in a centrifuge." *Proc. of ICPMG '02*, St John's, Balkema, 163-168.

Tsukamoto, Y., Ishihara, K. Nakazawa, H., Kamada, K. and Huang, Y. (2002): Resistance of partially saturated sand to liquefaction with reference to longitudinal and shear wave velocities, *Soils and Foundations*, 42(6), 93-104.

Yoshimi, Y., Tanaka, K. and Tokimatsu, K.(1989): Liquefaction resistance of a partially saturated sand, *Soils and Foundations*, 29(3), 157-162.